Nanoscale Res Lett (2009) 4:1197–1208
DOI 10.1007/s11671-009-9377-8

NANO EXPRESS

Effect of Cationic Surfactant Head Groups on Synthesis, Growth and Agglomeration Behavior of ZnS Nanoparticles

S. K. Mehta · Sanjay Kumar · Savita Chaudhary · K. K. Bhasin

Received: 24 December 2008 / Accepted: 15 June 2009 / Published online: 1 July 2009

Abstract Colloidal nanodispersions of ZnS have been prepared using aqueous micellar solution of two cationic surfactants of trimethylammonium/pyridinium series with different head groups i.e., cetyltrimethylammonium chloride (CTAC) and cetyltrimethylpyridinium chloride (CPyC). The role of these surfactants in controlling size, agglomeration behavior and photophysical properties of ZnS nanoparticles has been discussed. UV–visible spectroscopy has been carried out for determination of optical band gap and size of ZnS nanoparticles. Transmission electron microscopy and dynamic light scattering were used to measure sizes and size distribution of ZnS nanoparticles. Powder X-ray analysis (Powder XRD) reveals the cubic structure of nanocrystallite in powdered sample. The photoluminescence emission band exhibits red shift for ZnS nanoparticles in CTAC compared to those in CPyC. The aggregation behavior in two surfactants has been compared using turbidity measurements after redispersing the nanoparticles in water. In situ evolution and growth of ZnS nanoparticles in two different surfactants have been compared through time-dependent absorption behavior and UV irradiation studies. Electrical conductivity measurements reveal that CPyC micelles better stabilize the nanoparticles than that of CTAC.

Keywords ZnS nanoparticles · CTAC · CPyC · Turbidity · UV irradiation · Photoluminescence · Redispersion

Electronic supplementary material The online version of this article (doi:10.1007/s11671-009-9377-8) contains supplementary material, which is available to authorized users.

S. K. Mehta (✉) · S. Kumar · S. Chaudhary · K. K. Bhasin
Department of Chemistry, Centre for Advanced Studies in Chemistry, Panjab University, Chandigarh 160014, India
e-mail: skmehta@pu.ac.in

Introduction

The synthesis of ultrafine semiconducting particles is of great technological and scientific interest due to their superior physical and optical properties. Zinc sulfide (ZnS) is an important wide band gap (3.60 eV) semiconductor and used as a key material for large range of applications [1–3]. Over the years, attempts have been made to prepare, stabilize and isolate homogeneously dispersed ZnS nanoparticles with and without capping agents [4–7]. When these clean nanoparticles aggregate, they lose their nanoscale sizes and corresponding properties. Therefore, in addition to tune particle size, a low degree of agglomeration and monodispered size distribution are desirable to enable homogeneous arrangement of particles. Due to partially satisfactory results, available methods still represents a major challenge to date and ultimate aim of the current research in material science is to understand the mechanisms that determine the crystal habitat and shape of the crystal. In last few years, extensive structural, kinetic and thermodynamic studies have been performed to explore the fundamental understanding of surfactant–water system including the effect of additives on micellization [8–10]. However, still there are conflicting opinions on some aspects particularly, the studies regarding factors controlling the synthesis and stabilization of nanoparticles in aqueous surfactant solutions. Therefore, it is quite difficult to scale up a general method for the nanoparticles synthesis using surfactants, because numerous parameters with different influences enter in to consideration, while studying a particular system.

One interesting aspect, which should be mainly considered, is directly related to particle size control by the adsorption of surfactant onto the particles surface. Among several methods to prevent self-aggregation of nanoparticles, coating with

surfactants, where one end of the surfactant chain is anchored to particle surface and other end is free, is simple and effective method to first give one dimensionally ordered self-assembly and then higher dimensional close-packed superlattice [11]. The surfactant coating on nanoparticles changes their aggregation behavior due to changed interparticle potential. Therefore, different types of surfactants, depending upon their molecular structures, may tune the interparticle interactions to different extent and hence have different tendency to prevent the nanoparticles aggregation. Apart from the synthesis purpose, surfactants have been used in association with nanoparticles for variety of studies [12, 13]. Zaman et al. [14] has investigated the interparticle forces and stability of silica dispersions in C_{12}TAB through turbidity and viscosity measurements. Keeping in view the importance of surfactant–nanoparticles system, it would be very interesting to know whether there is any influence of surfactant structure on size, shape, stability and other properties of nanoparticles. A comparative study of a particular system in different surfactants can provide a better insight into the nanoparticles stability and properties. Naskar et al. [15] compared effect of two nonionic surfactant stabilized emulsions on ZnS nanoparticles size. Shao et al. [16] studied the role of oleic acid and TOP on growth and agglomeration behavior of cobalt nanoparticles synthesized via thermal decomposition. However, there is hardly any report on the comparative studies of ZnS nanoparticles in cationic surfactants till date.

The present report explores the stabilization mechanism and other characteristics of ZnS nanoparticles in the aqueous micellar solution of cationic surfactants. Two cationic surfactants from quaternary ammonium series viz. cetyltrimethylammonium chloride (CTAC) and cetylpyridinium chloride (CPyC) have been used for the synthesis of ZnS nanoparticles. Figure 1 depicts the molecular structure of the amphiphiles, CTAC and CPyC, where hydrophilic ammonium and pyridinium groups act as 'polar head,' and the hydrophobic hydrocarbon chain of sixteen carbons acts as 'non-polar tail'. Both the surfactants chosen are having same hydrocarbon chain length (C_{16}) and counter ion (Cl^-), but different head groups. Various aspects related to synthesis and characterization of ZnS nanoparticles have been discussed and compared. The effect of type of surfactants (with different head group) on agglomeration behavior and photophysical properties of ZnS nanoparticles has also been analyzed.

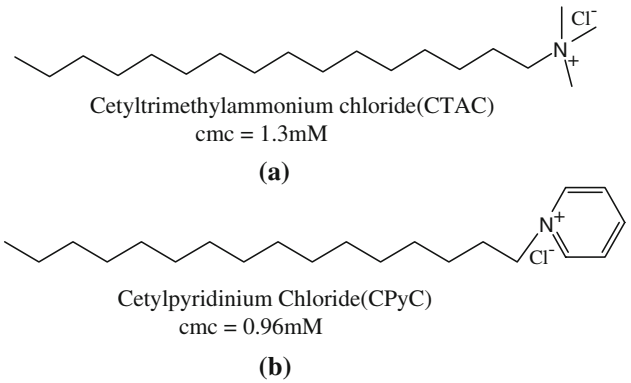

Fig. 1 Molecular structure of (**a**) CTAC and (**b**) CPyC

Materials and Methods

Chemicals

For the synthesis of ZnS nanoparticles, $Zn(OAc)_2{\cdot}2H_2O$ (99.5%), $Na_2S{\cdot}xH_2O$ (55–58% assay), all were of analytical grade obtained from central drug house (CDH). The surfactants, CTAC (99%) and CPyC (99%), were obtained from Fluka and Himedia, respectively. All reagents were used as received, without further purification. The solvents acetone and ethanol were AR grade products.

ZnS Nanoparticle Synthesis

Two micellar solutions of CTAC (3 mM), one containing $Zn(OAc)_2{\cdot}2H_2O$ (0.025 M) and another containing $Na_2S{\cdot}xH_2O$ (0.025 M), were prepared in double-distilled water. The synthesis of ZnS nanoparticles was performed by two-step procedure. The first step involves the generation of the S^{2-}-surfactant complex by adding aqueous sodium sulfide (0.025 M) to aqueous surfactant solutions. In the second step, dropwise addition of aqueous micellar solution containing $Zn(OAc)_2$ (0.025 M) into the above solution with constant stirring at ambient temperature leads to the formation of ZnS nanoparticles. The homogeneous solution was then allowed to stand for 30 min at room temperature. The dispersions were found to be stable for months together. The nanoparticles were separated by slow evaporation of solvent at 50–60 °C. The collected solid product was washed with double-distilled water and ethanol and then vacuum dried for 48 h. We also tried ultracentrifugation, but nanoparticles got badly agglomerated. Similar procedure was followed for the synthesis of ZnS nanoparticles in CPyC.

Characterization Methods

UV–vis Absorption Spectroscopy

Optical spectra of the nanodispersions were taken with a JASCO-530 V spectrophotometer in quartz cuvette of 1 cm path length. For time-dependent absorption measurements, two solutions were mixed and immediately

transferred to quartz cuvette. The mixing time was about 40–45 s before starting the absorbance measurement. The measurements were then taken at the rate of 12 measurements per minute. UV irradiation experiments were carried out in Popular India UV cabinet.

Electron Microscopy

Transmission electron microscopy (TEM) micrographs were taken using Hitachi (H-7500) transmission electron microscope operating at 80 kV. Samples for TEM studies were prepared by placing a drop of nanodispersion on a carbon-coated Cu grid, and the solvent was evaporated at room temperature. SEM images of powdered sample were taken using JEOL (JSM-6100) scanning microscope.

Dynamic Light Scattering

The dynamic light scattering (DLS) measurements were taken on ALV-5000 with Nd:YAG laser with a wavelength of 532 nm. Multiple tau digital correlation was measured at the minimum sampling of 6.25 ns using a dual auto correlation mode on an ALV-5000 correlator board. All measurements were taken at scattering angle of 90° for different suspensions. A sample cell was set in the toluene bath for index matching with the quartz. The temperature was maintained at 25 °C in the toluene bath.

X-Ray Diffraction Studies

Powder XRD studies were carried out using Panalytical, D/Max-2500 X-Ray Diffractometer equipped with Cu-kα radiation ($\lambda = 1.5418$ Å) employing a scanning rate of $0.02°\ s^{-1}$. Si was used as standard to determine the instrumental broadening, and the (111) reflection was analyzed. The $\Delta 2\theta$ for the silicon peak was about 0.06 (θ), and a simple instrumental correction was carried out by subtracting this value from the $\Delta 2\theta$ values corresponding to the diffraction peaks obtained for our samples.

FTIR Spectroscopy

FTIR spectra of dried ZnS nanoparticles were recorded with Perkin Elmer RX-1 spectrophotometer in frequency range of 4,000–900 cm^{-1}. Small amount of sample was mixed with 2–3 drops of CCl_4 to form a thick paste. The paste was then applied on NaCl plates to record the spectra.

Photoluminescence Spectroscopy

The PL spectra were recorded on Varian fluorescence spectrophotometer. The excitation wavelength of 320 nm was used, and PL emission was recorded in 330–560 nm range.

Turbidity Measurements

Turbidity measurements of redispersed ZnS nanopowder were taken in a digital turbidity meter (Decibel Instruments) with an accuracy of ±3% of full-scale deflection. Powdered ZnS nanoparticles (0.04 g) were dispersed in 35 mL water and sonicated for 30 min, then kept undisturbed in glass cuvette in the cuvette holder of turbidity meter. Turbidity of solution (in NTU) was noted after regular intervals.

Conductivity Measurements

The specific conductivity measurements of aqueous surfactant solutions in the presence of ZnS nanoparticles were measured using PICO digital conductivity meter operating at 50 Hz from Lab India instruments with an absolute accuracy of ±3%. Platinised platinum electrode was inserted in a double-walled vessel containing the solution in which the thermostated water was circulated. The conductivity cell was calibrated with standard KCl solutions, and the obtained cell constant was 1.02 cm^{-1}.

Results and Discussion

Formation of ZnS Nanoparticles and Optical Characterization

The formation of ZnS nanoparticles can be represented as of elementary ionic reaction

$$Zn^{2+}\ (\text{aqueous micelle}) + S^{2-}\ (\text{aqueous micelle}) \rightarrow ZnS(\text{NPs}).$$

Theoretically, the ratio $[Zn(OAc)_2]$:$[Na_2S]$ required seems to be 1:1. But actually $[S^{2-}] < [Na_2S]$, because aqueous solution of Na_2S contained both aqueous H_2S and HS^- and other sulfur oxyions such as thiosulfate and sulfite, originating either as impurities in solid Na_2S or from rapid oxidation of HS^- by O_2 [17]. Based on the test experimental results, the ratio $[Zn(OAc)_2]$:$[Na_2S] = 1:2$ was found to be the optimum. The volume of the solutions was adjusted so as to get final concentration, $[Zn(OAc)_2] = 2$ mM. The adsorption of surfactant molecules onto the particles surface restricts their unlimited growth. The particle size was further tailored by using two surfactants with different head group, keeping other parameters unaltered. To investigate the optical properties of as-prepared ZnS nanoparticles dispersed in aqueous micellar solution of CTAC and CPyC, UV–vis absorption spectra were recorded as shown in Fig. 2a. Both

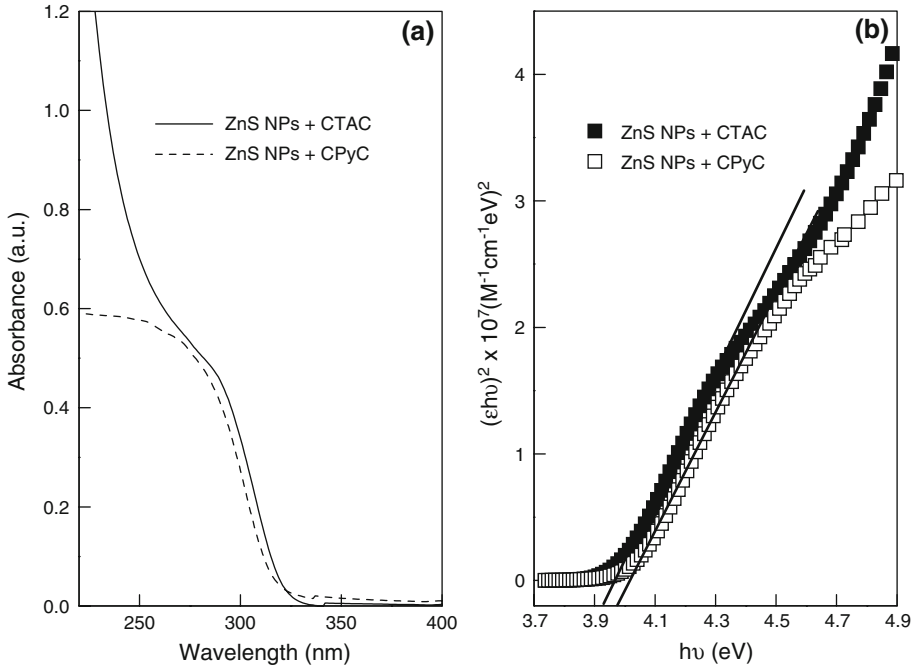

Fig. 2 (**a**) Absorption spectra of as-prepared ZnS nanoparticles in aqueous micellar solution CTAC and CPyC. (**b**) Respective Tauc plots for the determination of the band gap of ZnS nanoparticles

the curves exhibit well-defined absorption shoulder with band edge located at 326 nm in CTAC and at 318 nm in CPyC, which are considerably blue shifted as compared to bulk ZnS (340 nm) due to quantum confinement of ZnS nanoparticles [18]. The optical band gap of the nanoparticles has been evaluated from the Tauc relation [19].

$$(\varepsilon h\nu) = C(h\nu - E_g)^m \quad (1)$$

where C is a constant, ε is molar extinction coefficient, E_g is optical band gap of the material and m depends on the type of transition. The value of molar extinction coefficient for the synthesized nanoparticles is more than 900; thus, we can assume that the transitions in the nanocrystals are allowed direct transitions [20]. For $m = ½$, $E._g$ in Eq. 1 is directly allowed band gap. The optical band gap was estimated from the linear portion of the $(\varepsilon h\nu)^2$ versus $h\nu$ plots shown in Fig. 2b. From Tauc plots, optical band gap values for ZnS nanoparticles prepared in CTAC and CPyC were estimated to be 3.92 ± 0.01 and 3.98 ± 0.01 eV, respectively. From the band gap values, the sizes of nanoparticles calculated using Wang equation [21] were found to be 6.55 ± 0.05 nm in CTAC and 5.90 ± 0.05 nm in CPyC, respectively.

Electron Microscopy and DLS

The average particle size and size distribution were estimated by the combination of TEM and DLS analysis. Figure 3 shows the representative TEM images of ZnS nanoparticles prepared in CTAC and CPyC micellar media and their respective DLS plots. As evident from the images, the particles are roughly spherical in shape and polydispersed with average particle size in the range of 3–8 nm. Few particles tend to form irregular aggregates, which are seen as large particles in both the images. However, it was observed that ZnS particles prepared in the presence of CTAC have greater agglomeration tendency (Fig. 3a) when compared to those prepared in CPyC. Furthermore, DLS clearly shows narrow size distribution of ZnS nanoparticles in CPyC when compared to that in CTAC with diameters in the range 5–21 ± 2 nm and 4–63 ± 3 nm, respectively. The intensity-weighed analysis indicates that most of the ZnS nanoparticles in aqueous micellar solution of CTAC and CPyC have a diameter of 9 ± 3 nm and 7 ± 3 nm, respectively. The range of sizes estimated from UV–vis spectroscopy, TEM and DLS can be considered to be in good agreement, although the three techniques analyze particle sizes differently. DLS analyses include the surfactant shell and determine hydrodynamic size, UV–vis analyses include quantum mechanical calculations based on light absorption; whereas using TEM we can directly look at ZnS core. The surface morphology of washed and dried samples prepared in aqueous micellar solution of CTAC and CPyC was studied by using a scanning electron microscope (SEM). Figure S1 (supplementary material) shows the SEM micrographs of ZnS nanoparticles separated from CTAC and CPyC micellar solution. It shows that the particles are roughly spherical in shape.

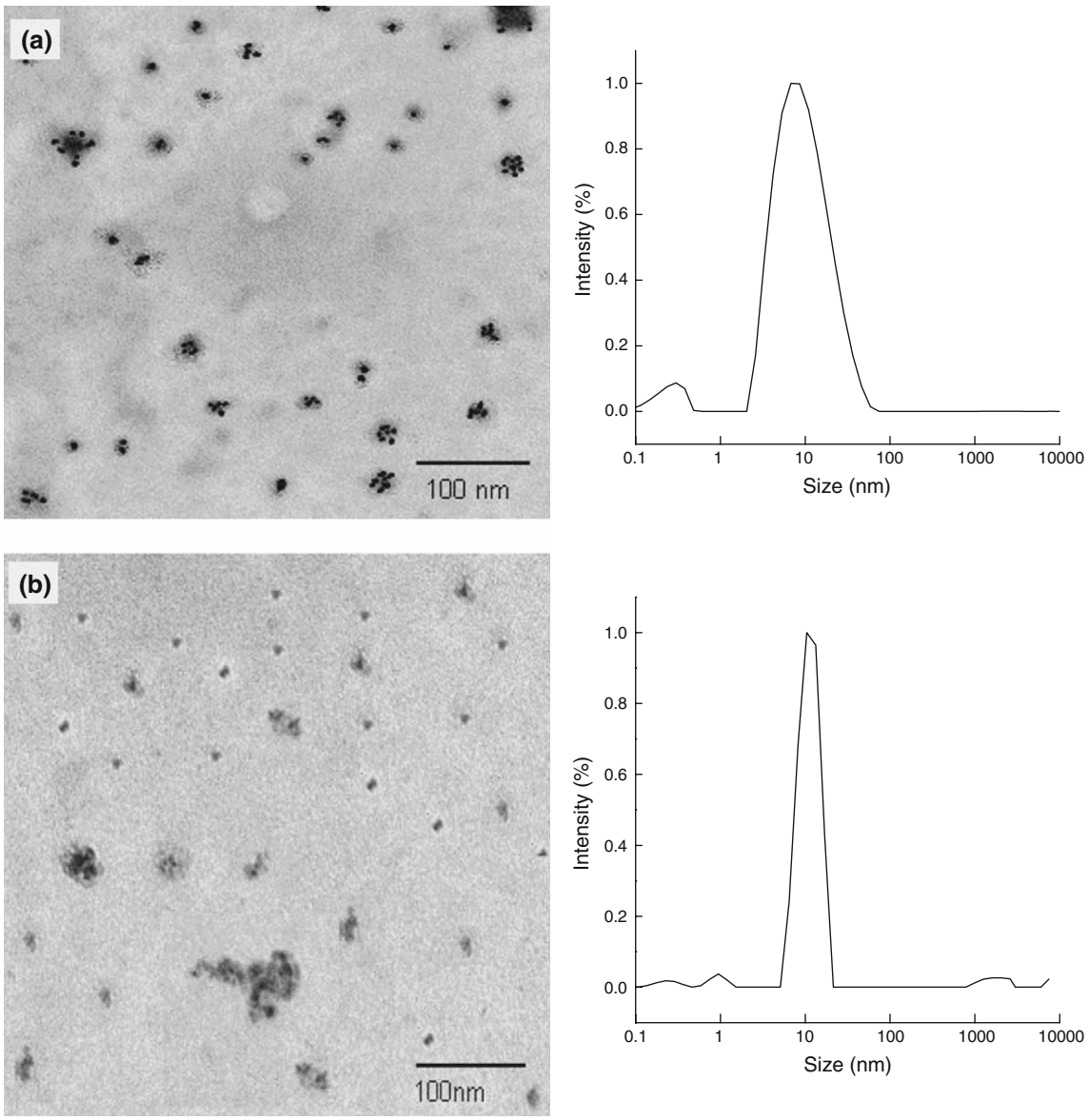

Fig. 3 TEM micrographs and intensity-weighed size distribution using DLS of the ZnS nanoparticles prepared in 3 mM aqueous solution of (**a**) CTAC and (**b**) CPyC

X-Ray Diffraction Studies

To investigate the crystalline structure of the product, powder XRD measurements were taken at room temperature. The X-ray diffraction patterns of powdered ZnS nanoparticles prepared in CTAC and CPyC are shown in Fig. 4, and the peaks are well indexed into pure zinc blend structure (JCPDS powder diffraction file no. 5-0566). Three diffraction peaks observed at 28.5°, 47.6° and 56.4° in both the samples corresponds to (111), (220) and (311) planes, respectively. The broadening of powder XRD peaks indicates that the particle sizes are in nanometer range. Clearly, the peaks in Fig. 4b are a little broader than that in Fig. 4a indicates that the particles prepared in presence of CPyC are slightly smaller when compared to those prepared in CTAC. The average crystallite size was determined from the full width at half maxima (FWHM) of the diffraction peaks using Debye-Scherrer formula [22].

$$D = \frac{\alpha\lambda}{\beta Cos\theta} \tag{2}$$

where D is mean crystallite diameter, α is a geometrical factor ($\alpha = 0.94$), λ is the wavelength of X-rays used for analysis and β is full width at half maxima (FWHM) of peaks. Here, θ corresponding to (111) reflections of powder XRD pattern have been used to calculate the nanoparticle size. In almost all cases, line broadening occurs due to simultaneous size and strain effects [23]. Therefore, we

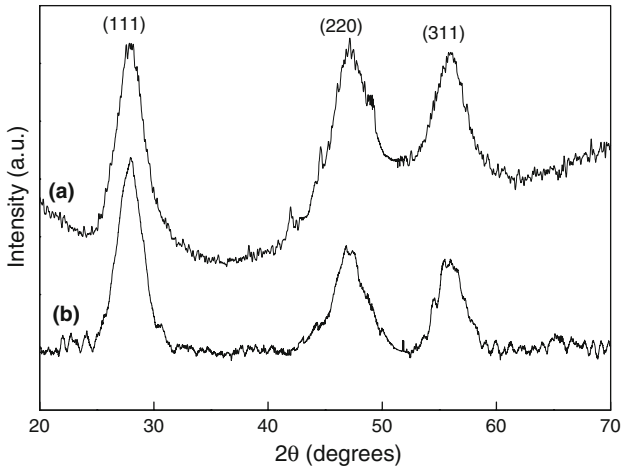

Fig. 4 Powder XRD patterns of the powdered ZnS nanoparticle prepared in (**a**) CTAC and (**b**) CPyC

have also used another method, i.e., the Williamson-Hall plots to separate the contribution due to strain (ε) and crystallite size (D) toward line broadening. The Williamson-Hall equation is expressed as follows [24]:

$$\beta Cos\theta = \frac{\alpha\lambda}{D} + 2\varepsilon Sin\theta \quad (3)$$

Figure 5 represents the plot of $\beta Cos\theta$ versus $2Sin\theta$. The slope of the linear fit gives the amount of strain, and from the intercept on $\beta Cos\theta$ axis, crystallite size can be calculated. The average crystallite sizes and amount of strain calculated on the basis of powder XRD analysis of ZnS nanoparticles synthesized in CTAC and CPyC are presented in Table 1. The powder XRD analysis reveal that

Table 1 Average crystallite sizes and amount of strain of ZnS nanoparticles calculated on the basis of powder XRD analysis

Surfactant	D_S (nm)	D_{WH} (nm)	Strain ($\times 10^{-3}$)
CTAC	11.0 ± 0.2	13.4 ± 0.3	4.6 ± 0.6
CPyC	10.8 ± 0.2	13.1 ± 0.3	4.3 ± 0.6

D_S, crystallite diameter calculated from Debye-Scherrer formula; D_{WH}, crystallite diameter calculated from Williamson-Hall plots

during separation and drying process particles grew and size became almost double when compared to that calculated on the basis of UV absorption spectra in both the surfactants.

Turbidity Measurements

Turbidity is an expression of optical property that uses light scattering properties of suspensions in the sample. The stability of powdered ZnS nanoparticles, when redispersed in water, has been studied using turbidity measurements. We have also tried other organic solvents for redispersion studies, but particles settled down within 5–10 min. As the particles settled down turbidity goes on decreasing, and this decrease in the turbidity value with time can be used to calculate the fraction of particles that remains suspended in water for long time. The turbidity results for ZnS nanoparticles prepared in CTAC and CPyC are presented in Fig. 6. Initially, a sharp decrease in turbidity was observed because the bigger particles settled down immediately. On the basis of decrease in turbidity values, it was calculated

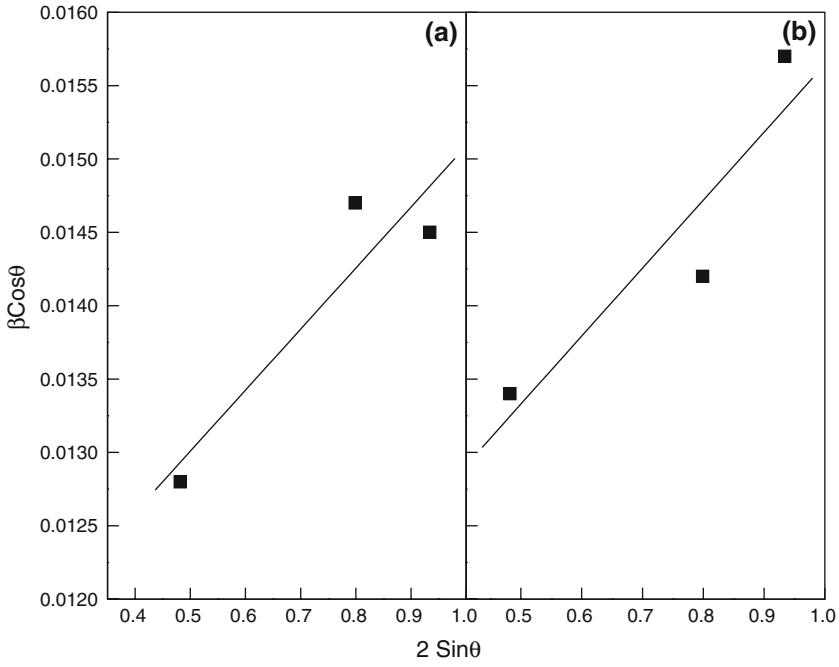

Fig. 5 Williamson-Hall plots of powder XRD data of ZnS nanoparticles prepared in (**a**) CTAC and (**b**) CPyC

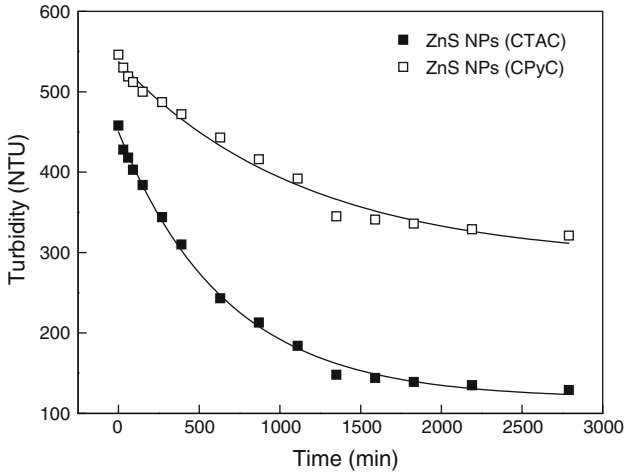

Fig. 6 Decrease in turbidity of ZnS nanoparticles (redispersed in water) as a function of time

that 22.5% particles in CTAC and 20.4% in CPyC settled down with in 2.5 h. Clearly, both the samples show exponential decrease in turbidity, and decay was found to be more rapid for ZnS nanoparticles prepared in CTAC than those prepared in CPyC. Calculations based up on decrease in turbidity values show that after 60 h, about 58.7% nanoparticles prepared in CPyC remained suspended in water when compared to only 28.2% of those prepared in CTAC.

The turbidity results therefore reveal that ZnS nanoparticles prepared in aqueous micellar solution of CPyC do not form permanent aggregates during separation and drying process and have good redispersion tendency when compared to those prepared in aqueous micellar solution of CTAC. It can be thought that the adsorbed surfactant molecules remained intercalated between the particles during separation and drying process, preventing their permanent fusion to form bigger particles and get redispersed when dissolved in water. The presence of surfactant molecules in powdered nanoparticles has also been evidenced from FTIR studies.

FTIR Analysis

The mode of anchoring of CTAC and CPyC onto the surface of synthesized ZnS nanoparticles was examined by recording their FTIR spectra. The FTIR spectra of pure surfactant and solid capped samples prepared in aqueous micellar solution of CTAC and CPyC are given in Fig. 7. Clearly, a broad peak at 3,400–3,430 cm^{-1} due to O–H stretching has been observed in all the samples because of some absorbed moisture. By comparing these spectra with that of pure surfactants, it was found that there has been significant shift in peaks due to –C–N stretching, –C–H scissoring vibrations of $–N–CH_3$ moiety and –C=C– stretching in pyridinium ring in the presence of ZnS.

However, the peaks due to –C–H stretching of hydrocarbon tail remained unaffected. The detailed assignment of FTIR peaks of CTAC and CPyC in the presence and absence of ZnS nanoparticles are given in Table 2 [25–27]. These observations reveal that in both the cases capping of nanoparticles was due to adsorption of surfactant molecules through head groups. Hence, the surface passivation of ZnS nanoparticles by surfactant adsorption makes them

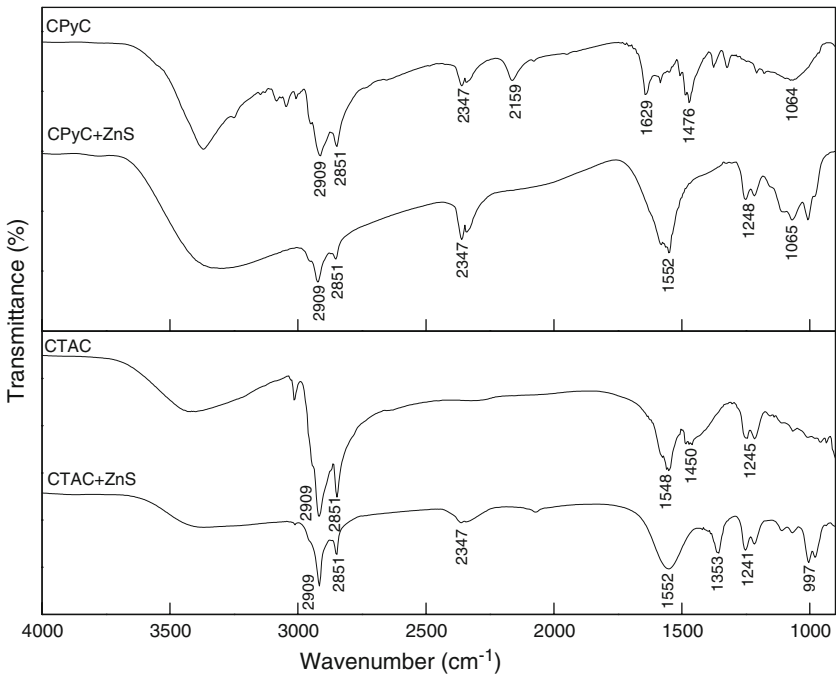

Fig. 7 FTIR spectrum of pure surfactants and ZnS nanoparticles prepared in CPyC and CTAC

Table 2 Assignment of FTIR peaks of CTAC and CPyC capped ZnS nanoparticles

Peak assignment	Peak position (cm^{-1})			
	CTAC	CTAC + ZnS NPs	CPyC	CPyC + ZnS NPs
$\upsilon_A(-CH_2)$	2,909	2,910	2,913	2,914
$\upsilon_S(-CH_2)$	2,850	2,851	2,849	2,848
$\upsilon_{Anti}(CO_2)$	2,347	2,347	2,347	2,348
$\upsilon_{Py}(C=C)$	–	–	1,629	–
$\delta_S(-C-H)$	1,542, 1,470	1,552	1,466	1,552
$\upsilon_{Ar}(C=C,C-N)$	–	–	1,373, 1,315	1,353
$\upsilon_{Str}(C-N, C-C)$	1,243, 1,215	1,248	1,245	1,241
$\upsilon_R(-CH_2)$	985	1,065	1,067	997

υ_A, asymmetric stretching; υ_S, symmetric stretching; υ_{Anti}, antisymmetric stretching; υ_{Py}, lewis-bonded pyridine; δ_S, scissoring; υ_{Ar}, aromatic; υ_R, rocking

aggregation resistant. Furthermore, the peak –C=C– stretching in lewis-bonded pyridinium (1629 cm^{-1}) has been completely diminished in the presence of nanoparticles showing stronger adsorption of CPyC onto the particles surface when compared to that of CTAC.

Photoluminescence Studies

The photoluminescence (PL) emission is one of the most important physical properties in ZnS nanoparticles and depends upon synthesis conditions, shape, size and energetic position of the surface states [28–30]. The photoluminescence spectra of as-prepared ZnS nanoparticles in aqueous micellar solution of CTAC and CPyC are presented in Fig. 8. In both the samples, excitation wavelength of 320 nm was used. PL spectra of aqueous surfactant solutions without nanoparticles were also recorded and showed no emission at same excitation. Dangling bonds [31] are found on the surface of most crystalline materials due to the absence of lattice atoms above them. The surface tends to reconstruct or adsorb some other species to reduce the surface energy. The emission band at 359 and 352 nm for the samples prepared in CTAC and CPyC, respectively, may be due to the dangling bond of cationic surfactant head group linked with S^{2-} at ZnS nanoparticle surface [31]. The red shift in emission peak at 359 nm for ZnS prepared in CTAC compared to that of at 352 nm for CPyC capped nanoparticles explains the formation of smaller-sized ZnS nanoparticles in CPyC.

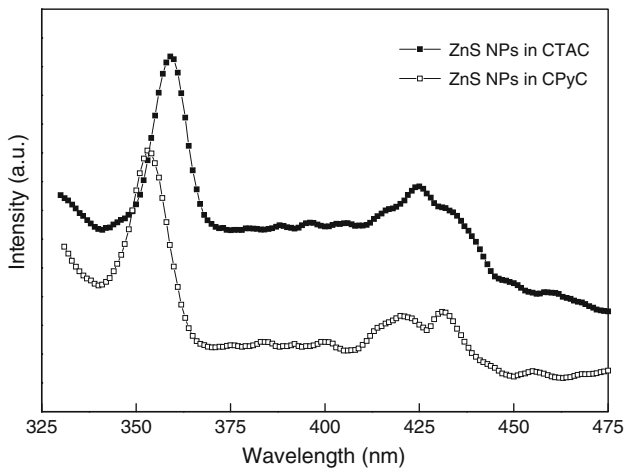

Fig. 8 PL spectra of ZnS nanoparticles prepared in aqueous micellar solution of CTAC and CPyC

The synthesized ZnS nanoparticles are found to have cubic crystal lattice, and Schottky defects are dominant in cubic ZnS [32]. Therefore, deep traps in cubic ZnS involve Zn^{2+} and S^{2-} vacancies. The broad, low intense, deep trap emission band at ~424 nm reveals few defects in the synthesized nanoparticles in both the surfactants [33]. Furthermore, the narrow emission band indicates the formation of nanoparticles with narrow size distribution [34]. The PL intensity of ZnS nanoparticles prepared in CPyC was found to be less, because of the interactions between pyridine and surface point defects of ZnS nanoparticles. The CPyC is effective in quenching the luminescence [31] due to the ability of N-atom in pyridinium cation to seize the electrons from the surface states of nanoparticles making the electron transfer easy. These results indicate that the photophysical properties of ZnS nanoparticles depend up on the size and surface passivation, which might help to further understand the physical mechanism of ZnS nanoparticles that give rise to PL properties.

Kinetics of Particle Formation

The process of nucleation and growth during particle formation in two surfactants was monitored using UV–vis spectroscopy. The UV absorbance is a function of concentration and size of nanoparticles. Therefore, time-dependent absorption of ZnS nanoparticles can be used to compare the evolution and growth of nanoparticles in the

presence of the surfactants. The shoulder at 294 nm in UV–vis spectra (Fig. 2) is characteristic for ZnS nanoparticles. Any change in its position and absorbance can be taken as an indicative of growth process. The growth-dependent shift in UV–vis spectra of as-prepared ZnS nanoparticles in aqueous CPyC and CTAC as a function of time elapsed after the reaction starts has been represented in Fig. S3 (supplementary material). Ten spectra of ZnS nanoparticles in each surfactant were recorded at an interval of 2 min. The typical shoulder due to ZnS has progressively red shifted with time, and the red shifts become very small after 20 min in both the surfactants (Fig. S3). The absorbance of the shoulder also follows nearly same trend. To confirm this behavior, the time evolution of the absorbance at 294 nm for ZnS nanoparticles in aqueous solution of CTAC and CPyC was also monitored, and the results are shown in Fig. 9. In this experiment, the particles were produced by quickly adding the aqueous micellar solution containing Zn^{2+} in to those having S^{2-} ions. The resultant solution was then immediately transferred to quartz cuvette for absorbance measurements at fixed wavelength of 294 nm. The mixing time was about 40–45 s before starting the absorbance measurement. Therefore, time 'zero' was on the order of 40–45 s after mixing. The reaction was monitored for 100 min. It can be observed that the nucleation takes place very rapidly (within 40–45 s) in both the surfactants, and then growth rate goes on decreasing with time (Fig. 9). The red shift in the spectra (Fig. S3) can be interpreted in terms of a growing process of the ZnS nanoparticles and increase in absorbance as increase in concentration of absorbing ZnS nanoparticles. Moreover, the red shift has only been observed in 260–300 nm region and not in the whole of the spectra. This means that during growth process the particle sizes of some particles increase producing more number of particles that absorb in 260–300 nm region only. Interestingly, in the presence of CPyC, the absorbance decreases after reaching a plateau region of maximum value within 15–20 min (Fig. 9). This decrease in absorbance has been attributed to UV-induced photodegradation of ZnS nanoparticles [35].

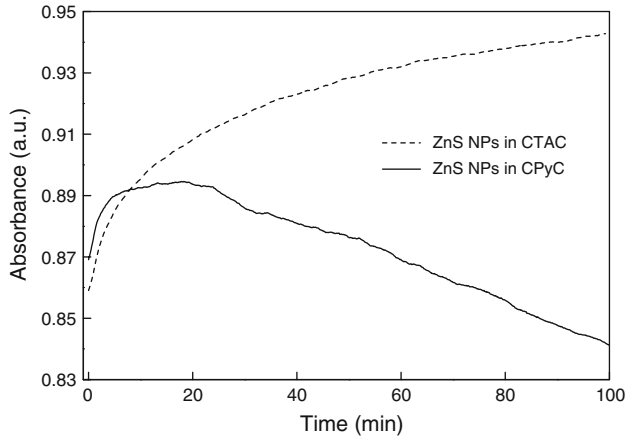

Fig. 9 UV absorbance of as-prepared ZnS nanoparticles in aqueous solution of CTAC and CPyC measured at 294 nm as function of time

However, decrease in absorbance was not observed for ZnS nanoparticles synthesized in the presence of CTAC. At first sight, ZnS nanoparticles in CTAC seem to be resistant toward UV-induced degradation. However, CTAC cannot shield the ZnS nanoparticles from UV light, as it does not absorb the UV light. To further confirm this behavior, UV irradiation studies were carried out on ZnS nanoparticles for different durations in both the surfactants at an irradiation wavelength of 254 nm, and the observations are presented in Fig. 10. It is clear that the reverse phenomenon of the growth process observed in Fig. S3 has happened i.e., UV light degrades the particles leading to decrease in their size that causes blue shift in the spectra. In addition, according to Lambert–Beer law for quantitative determination of concentrations of the absorbing species in solution, the absorbance is directly proportional to the concentration of absorbing species i.e., concentration of ZnS nanoparticles in this particular case. To support this view, UV–vis spectra of ZnS nanoparticles at different concentrations were also recorded in both the surfactants (Fig. S4, supplementary material). It shows a decrease in absorbance with decrease in the concentration of ZnS nanoparticles. Therefore, the small blue shift in absorption shoulder and decrease in absorbance with irradiation time confirm that some of the ZnS nanoparticles become smaller, and the concentration of absorbing particles decreases in both the surfactants.

Although UV light affects ZnS nanoparticles in both the surfactants; however, the effect seems to be more pronounced in CPyC than in CTAC. The growth of ZnS nanoparticles and the degrading effect of UV light can be correlated to explain the resultant evolution of ZnS nanoparticles in aqueous micellar solutions as:

(1) The growth of ZnS nanoparticles in CTAC is faster than UV-induced decay, and resultant effect seems to increase in absorbance only. On the other hand, in the presence of CPyC, nanoparticles growth is slow and decreases with time. At one stage, the nanoparticles growth becomes so slow that UV-induced decay overcomes the growth, and overall effect remains decay only.

(2) The UV light can degrade the nanosized particles much faster due to their large surface area [36]. The fast growth in the case of CTAC leads to larger size particles (small surface area) and, therefore, UV light-induced decay is slow when compared to growth. On the other hand, in CPyC, the surfactant molecules

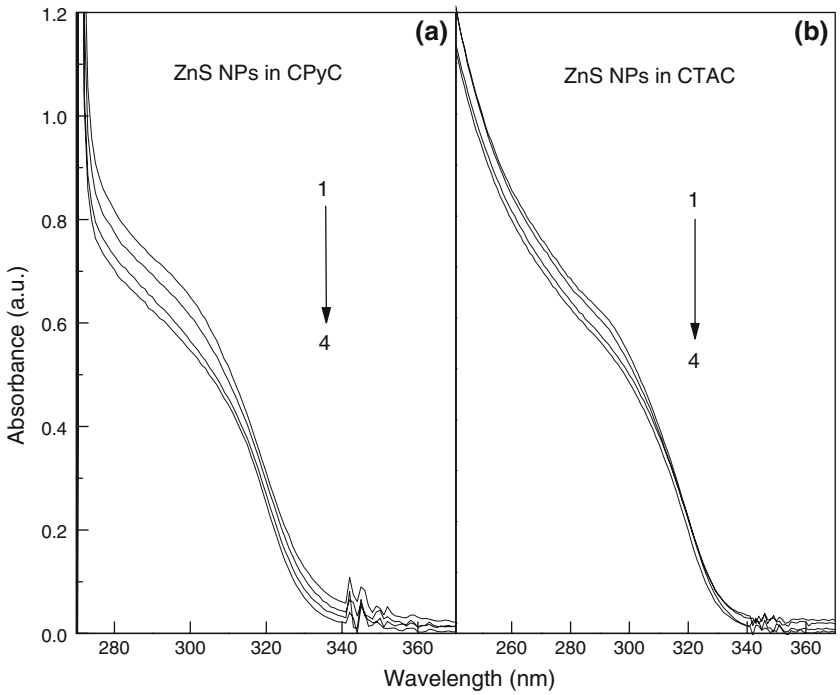

Fig. 10 Absorption spectra of ZnS nanoparticles in (**a**) CPyC and (**b**) CTAC after UV irradiation at 254 nm for (*1*) 0 h, (*2*) 1 h, (*3*) 2 h and (*4*) 3 h

stabilize the particles at small size (large surface area), and hence the particles are more prone to decay due to their large exposed surface area to UV light. Even some of the small particles disappeared leading to decrease in absorbance. In addition, the head group area of CPyC is more when compared to that of CTAC [37, 38]. Therefore, the particles could not grow and got stabilized at smaller size due to adsorption of large head group of CPyC.

Furthermore, the effect of UV radiation of two different wavelengths (254 and 365 nm) on ZnS nanoparticles has also been investigated. The plots are shown in Fig. S2 (supplementary material). The results depict that short wavelength or high energy radiations degrade the nanoparticle to a larger extent than longer wavelength (low energy) radiations irrespective of the nature of surfactants.

Aggregation Behavior of Surfactants in Presence of ZnS Nanoparticles

The aggregation behavior of both the surfactants in the presence of respective nanoparticles has also been studied. When dissolved in water at a concentration below critical micellar concentration (cmc), the surfactant behaves as a strong electrolyte, whereas above the cmc, the monomers form aggregates called micelles. The process of aggregation is affected due to temperature, solvents and presence of any other external entity.

The physical properties of surfactants such as conductivity, viscosity, surface tension, osmotic pressure and turbidity, etc., when plotted as a function of concentration, show a break and any of these can be used to determine the cmc [39]. Here, electrical conductivity method has been used to study the aggregation behavior of surfactant in the presence of ZnS nanoparticles prepared in respective surfactants. The changes in conductivity were measured during titration of surfactant into 5 mM aqueous ZnS solution at 298.15 K, and the results are presented in Fig. 11. The overall increase in conductivity of surfactants in the studied range is due to conducting nature of charged nanoparticles dispersed in surfactant solution. In the presence of ZnS nanoparticles, the process of micellization takes place prior to that of free micelles. The decrease in cmc values of the surfactants in the presence of some additives has been attributed to the screening of surface charge of micelles [39]. The decrease in cmc values in the presence of ZnS nanoparticles indicates that the presence of nanoparticles provides the driving force for micellization. Therefore, micellization is expected to takes place earlier than in free micelles. The driving force for early micellization may be due to the screening of surface charge; however, more detailed investigation is required to validate such interesting behaviors and hypothesis.

Figure 11a depicts that ZnS nanoparticles (synthesized in CTAC) are better dispersed in aqueous solution of CTAC until cmc. After that nanoparticles settled down, and CTAC micelles behave like that of pure CTAC. It indicates that soon after the formation CTAC micelles, the ZnS nanoparticles agglomerates and settles down. However, in aqueous solution of CPyC in the presence of nanoparticles, the nature of conductivity curves remains same even after

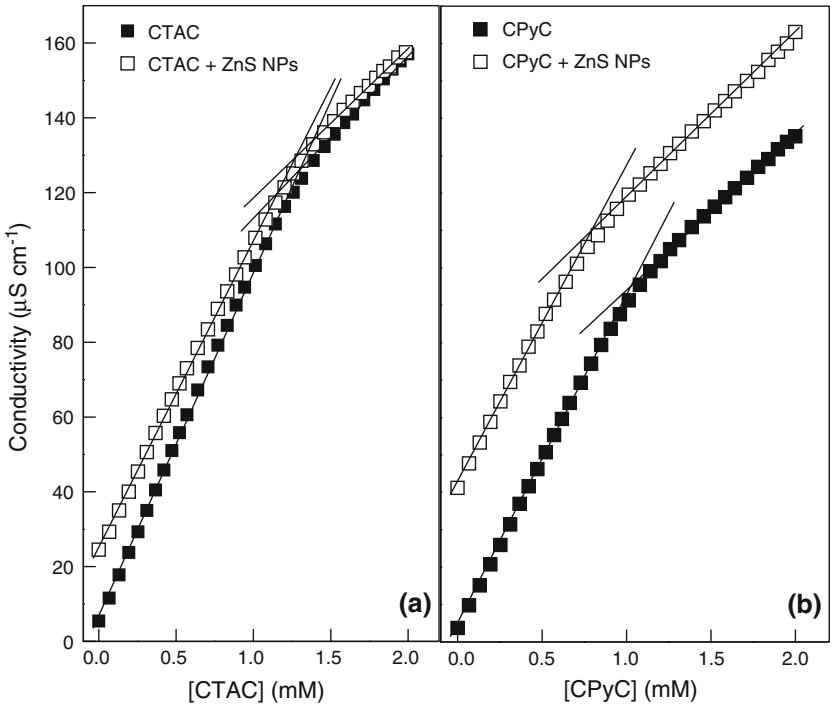

Fig. 11 Conductometric studies on aggregation of (**a**) CTAC and (**b**) CPyC in the presence of ZnS nanoparticles prepared in respective surfactants

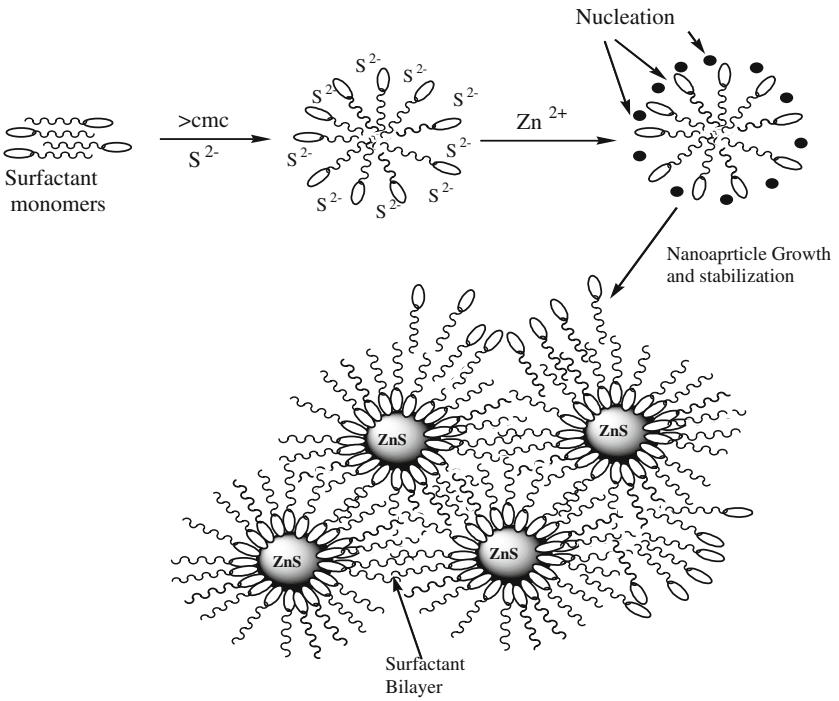

Fig. 12 Scheme of the ZnS nanoparticle formation in aqueous micellar solution of cationic surfactants (pictorial representation not to the scale, actual size of surfactant is very small when compared to ZnS nanoparticles)

cmc because of the fact that ZnS nanoparticle (synthesized in CPyC) remained suspended even after formation of micelles. This is due to more electrostatic attraction provided by larger head group size of CPyC for the stabilization of nanoparticles. The conductivity studies, thus, reveal that CPyC micelles solubilized the nanoparticles better when compared to CTAC micelles.

Furthermore, the pH of the prepared ZnS colloidal solution in the presence of CTAC and CPyC was also measured and found to be 6.26 and 6.07, respectively. Zhang et al. [17] have explained that ZnS particles are negatively charged in the pH range of $5.3 < \text{pH} < 9.3$, and negatively charged species such as Br^- or HS^- face an electrostatic barrier to surface adsorption. Therefore, we

hypothesize that synthesized particles are negatively charged due to excess S^{2-} ions on the particle surface and draw the cationic surfactant unimers via long-range electrostatic forces that induce the surfactant adsorption through head group. This is also supported by FTIR and fluorescence results. The hydrophobic tail region, in principle, cannot prefer the aqueous environment, and thus a counter layer is oriented in opposite way resulting in interpenetration of the surfactant hydrophobic tails between two layers with hydrophilic groups headed outward. The head group of this counter layer can be the part of adsorbed layer of other ZnS nanoparticle, thus giving a surfactant nanoparticles network structure in solution. On the basis of above discussion, the probable schematic representation of ZnS nanoparticle formation in aqueous micellar media of cationic surfactant has been presented in Fig. 12.

Conclusions

The ZnS nanoparticles have been prepared in aqueous micellar solution of two cationic surfactants viz. CTAC and CPyC having different hydrophilic head groups. The studies reveal that the stabilization and agglomeration of ZnS nanoparticles in aqueous micellar media depends up on surfactant head group. Based on UV–vis and turbidity experiments, CPyC has been found to provide better stabilization when compared to that by CTAC. Dependence of photoluminescence emission on the size and surface passivation of nanoparticles has also established. The studies on dependence of photophysical properties of ZnS nanoparticles on surfactant head group will be helpful in defining its priorities for optical applications.

Acknowledgments Sanjay Kumar is thankful to CSIR, Government of India for Junior Research Fellowship. Financial assistance from DST is gratefully acknowledged.

References

1. H. Yang, P.H. Holloway, J. Phys. Chem. B **107**, 9705 (2003)
2. N. Karar, S. Raj, F. Singh, J. Cryst. Growth **268**, 585 (2004)
3. W. Chen, A.G. Joly, J.O. Malam, J.O. Bovin, J. Appl. Phys. **95**, 667 (2004)
4. C. Yang, Y. Liu, H. Sun, D. Guo, X. Li, W. Li, B. Liu, X. Zhang, Nanotechnology **19**, 095704 (2008)
5. S. Biswas, S. Kar, Nanotechnology **19**, 045710 (2008)
6. P.S. Khiew, S. Radiman, N.M. Huang, Md.S. Ahmed, K. Nadarajah, Mat. Lett. **59**, 989 (2005)
7. S. Wajeh, Z.S. Ling, X. Xu-Rong, J. Cryst. Growth **255**, 332 (2003)
8. A.J.M. Valente, H.D. Burrows, R.F. Pereira, A.C.F. Ribeiro, J.L.G. Costa Pereira, V.M.M. Lobo, Langmuir **22**, 5625 (2006)
9. J. Du, B. Jiang, J. Xie, X. Zeng, J. Disp. Sci. Technol. **22**, 529 (2001)
10. L. Yu, T. Lu, Y.X. Luan, J. Liu, G.Y. Xu, Colloid Surf. A **257**, 375 (2005)
11. J.C. Wang, P. Neogi, D. Forciniti, J. Chem. Phys. **125**, 194717 (2006)
12. V.C. Moore, M.S. Strano, E.H. Haroz, R.H. Hauge, R.E. Smally, Nanoletters **3**, 1379 (2003)
13. H. Ma, M. Luo, L.L. Dai, Phys. Chem. Chem. Phys. **10**, 2207 (2008)
14. A.A. Zaman, P. Singh, B.M. Moudgil, J. Colloid Interface Sci. **251**, 381 (2002)
15. M.K. Naskar, A. Patra, M. Chatterjee, J. Collod Interface Sci. **297**, 271 (2006)
16. H. Shao, Y. Huang, H. Lee, Y.J. Suh, C.O. Kim, J. Appl. Phys. **99**, 08N702 (2006)
17. X.V. Zhang, S.P. Ellery, C.M. Friend, H.D. Holland, F.M. Michel, M.A.A. Schoonen, S.T. Martin, J. Photochem. Photobiol. A-Chem. **185**, 301 (2007)
18. L.E. Brus, J. Chem. Phys. **80**, 4403 (1984)
19. J. Tauc, A. Menth, J. Non-Cryst. Solids **8**, 569 (1972)
20. P. Mishra, M.A. Dubinskii, *UV-Spectroscopy and UV-Laser: Practical Spectroscopy Series*, vol. 30 (CRC Press, New York, 2002)
21. Y. Wang, A. Suna, W. Mahler, R. Kasowaki, J. Chem. Phys. **87**, 7315 (1987)
22. G. Schmid, *Nanoparticles: From Theory to Application* (Wiley, New York, 2004)
23. M.M. Savosta, V.N. Krivoruchko, I.A. Danilenko, V.Yu. Tarenkov, T.E. Konstantinova, A.V. Borodin, V.N. Varyukhin, Phys. Rev. B **69**, 024413 (2004)
24. G.K. Wiliamson, W.H. Hall, Acta Meatall. **1**, 22 (1953)
25. Z. Sui, X. Chen, L. Wang, Y. Chai, C. Yang, N. Zhao, Chem. Lett. **34**, 100 (2005)
26. G.T. Palomino, J.J.C. Pascual, M.R. Delado, J.V. Parva, C.O. Arean, Mater. Chem. Phys. **85**, 145 (2004)
27. R.A. Fogel, M.J. Rutherford, Am. Mineral. **75**, 1311 (1990)
28. W. Chen, Z.G. Wang, Z.J. Lin, L.Y. Lin, J. Appl. Phys. **82**, 3111 (1997)
29. T. Arai, T. Yoshida, T. Ogawa, J. Appl. Phys. **62**, 396 (1987)
30. M. Agata, H. Kurase, S. Hayashi, K. Yamamoto, Solid State Commun. **76**, 1061 (1990)
31. H. Tang, G. Xu, L. Weng, L. Pan, L. Wang, Acta Mater. **52**, 1489 (2004)
32. A.R. West, *Solid State Chemistry and its Applications* (Wiley, New York, 1984)
33. J.F. Suyver, S.F. Wuister, J.J. Kelly, A. Meijerink, Nano Lett. **1**, 429 (2001)
34. I.I. Yu, T. Isobe, M. Sennu, J. Phys. Chem. Solids **57**, 373 (1996)
35. A. Henglein, M. Gutierrez, Ber. Bunsenges Phys. Chem. **87**, 852 (1983)
36. U. Sohling, G. Jung, D.U. Saenger, S. Lu, B. Kutsch, M. Mennig, J. Sol Gel Sci. **13**, 685 (1998)
37. A.A. Atia, M.M. Saleh, J. Appl. Electrochem. **33**, 171 (2003)
38. F. Zhao, Y.K. Do, J.K. Xu, S.F. Liu, Colloid J. **68**, 784 (2006)
39. E.D. Goddard, K.P. Ananthapadmanabhan, *Interactions of Surfactants with Polymer and Proteins* (CRC Press, London, 1993), p. 20